

## **Comparison of retinal thickness by Fourier-domain optical coherence tomography and OCT retinal image analysis software segmentation analysis derived from Stratus optical coherence tomography images**

Erika Tátrai  
Sudarshan Ranganathan  
Mária Ferencz  
Delia Cabrera DeBuc  
Gábor Márk Somfai

# Comparison of retinal thickness by Fourier-domain optical coherence tomography and OCT retinal image analysis software segmentation analysis derived from Stratus optical coherence tomography images

Erika Tátrai,<sup>a</sup> Sudarshan Ranganathan,<sup>b</sup> Mária Ferencz,<sup>a</sup> Delia Cabrera DeBuc,<sup>b</sup> and Gábor Márk Somfai<sup>a</sup>

<sup>a</sup>Semmelweis University, Faculty of Medicine, Department of Ophthalmology, Mária Street 39, Budapest, 1085 Hungary

<sup>b</sup>University of Miami Miller School of Medicine, Bascom Palmer Eye Institute, 900 NW 17 Street, Miami, Florida 33136

**Abstract.** Purpose: To compare thickness measurements between Fourier-domain optical coherence tomography (FD-OCT) and time-domain OCT images analyzed with a custom-built OCT retinal image analysis software (OCTRIMA). Methods: Macular mapping (MM) by StratusOCT and MM5 and MM6 scanning protocols by an RTVue-100 FD-OCT device are performed on 11 subjects with no retinal pathology. Retinal thickness (RT) and the thickness of the ganglion cell complex (GCC) obtained with the MM6 protocol are compared for each early treatment diabetic retinopathy study (ETDRS)-like region with corresponding results obtained with OCTRIMA. RT results are compared by analysis of variance with Dunnett *post hoc* test, while GCC results are compared by paired t-test. Results: A high correlation is obtained for the RT between OCTRIMA and MM5 and MM6 protocols. In all regions, the StratusOCT provide the lowest RT values (mean difference  $43 \pm 8 \mu\text{m}$  compared to OCTRIMA, and  $42 \pm 14 \mu\text{m}$  compared to RTVue MM6). All RTVue GCC measurements were significantly thicker (mean difference between 6 and  $12 \mu\text{m}$ ) than the GCC measurements of OCTRIMA. Conclusion: High correspondence of RT measurements is obtained not only for RT but also for the segmentation of intraretinal layers between FD-OCT and StratusOCT-derived OCTRIMA analysis. However, a correction factor is required to compensate for OCT-specific differences to make measurements more comparable to any available OCT device. © 2011 Society of Photo-Optical Instrumentation Engineers (SPIE). [DOI: 10.1117/1.3573817]

Keywords: optical coherence tomography; image processing; segmentation algorithms; Fourier-domain optical coherence tomography; time-domain optical coherence tomography; retina.

Paper 10529R received Sep. 29, 2010; revised manuscript received Feb. 15, 2011; accepted for publication Mar. 14, 2011; published online May 6, 2011.

## 1 Introduction

Optical coherence tomography (OCT) is a noninvasive, noncontact diagnostic tool that provides cross-sectional imaging of the human eye *in vivo*.<sup>1</sup> Currently, the system in most widespread use is the third-generation time-domain (TD) StratusOCT (Carl Zeiss Meditec, Inc., Dublin, California), which has an axial resolution of  $10 \mu\text{m}$ .<sup>2</sup> Recently, the development of Fourier-domain OCT (FD-OCT) provides an imaging speed that is  $\sim 60$  times faster and a resolution that is up to five times higher compared to TD-OCT.<sup>3–6</sup> Many instruments from different manufacturers are now commercially available that incorporate FD-OCT technology, one of them being RTVue-100 FD-OCT (Optovue Inc., Fremont, California), which has an axial resolution of  $5 \mu\text{m}$ .<sup>2</sup> This device is able to measure total retinal thickness (RT) along with the thickness of the ganglion cell complex (GCC) in the macular area, the latter comprising the retinal nerve fiber layer, ganglion cell layer, and inner plexiform layer.

It is well known that StratusOCT algorithms are prone to segmentation errors and cannot provide quantitative information on intraretinal layers.<sup>7–11</sup> As a result, potentially useful

information is not extracted by StratusOCT. In an effort to provide additional retinal quantifications along with accurate automatic/semiautomatic detection, we analyzed the StratusOCT images with a software tool for OCT retinal image analysis (OCTRIMA), which is an interactive, user-friendly stand-alone application for analyzing StratusOCT retinal images. The OCTRIMA software integrates a novel denoising and edge-enhancement technique along with a segmentation algorithm developed by Cabrera Fernández *et al.*<sup>12</sup> Moreover, OCTRIMA is able to minimize segmentation errors, give quantitative information of intraretinal structures, and also facilitates the analysis of other retinal features that may be of diagnostic and prognostic value, such as morphology and reflectivity.<sup>13</sup> The OCTRIMA software enables the segmentation of seven cellular layers of the retina on OCT images based on their optical densities: the retinal nerve fiber layer, the ganglion cell and inner plexiform layer complex, the inner nuclear layer, the outer plexiform layer, the outer nuclear layer, the inner-outer photoreceptor junction (IS/OS), and retinal pigment epithelium (RPE). We have previously shown a high reliability and reproducibility of OCTRIMA software using StratusOCT data from normal healthy eyes.<sup>14,15</sup>

It is noteworthy that patients with dense cataract or retinal disease may have problems fixating, making it difficult to record

Address all correspondence to: Gábor Márk Somfai, Semmelweis University, Department of Ophthalmology, Mária Street 39, Budapest, 1085 Hungary; Tel: 3063266000; Fax: 3053453547; E-mail: somfaigm@yahoo.com.

high-quality OCT images for further analysis. As a matter of fact, one of the disadvantages of TD over FD-OCT is the potential occurrence of decentration artifacts,<sup>8</sup> which are common in StratusOCT images in elderly patients<sup>8</sup> because of the poor fixation cooperation. Thus, taking into account that image quality could be affected by media opacities,<sup>16,17</sup> it is important to consider the effect of dense optical media, such as cataracts, on thickness measurements and segmentation performance when comparing OCT data.

The main purpose of the present study is to compare RT and GCC thickness measurement calculations and segmentation performance between RTVue FD-OCT and OCTRIMA segmentation analysis derived from StratusOCT images. We also compare RT measurements between StratusOCT and RTVue, and StratusOCT and OCTRIMA. In addition, we review currently available data about the difference in RT measurements of commercially available FD-OCT devices.

## 2 Patients and Methods

A total of 11 eyes from 11 subjects (nine women and two men) were included in this study. Taking into consideration that image quality could be affected by media opacities,<sup>16,17</sup> we included elderly subjects each of whom underwent uneventful phacoemulsification surgery with posterior chamber lens implantation 6–12 months prior to enrollment. The mean patient age was  $70 \pm 7$  years (range, 65–88 years). Elderly subjects were included to provide a more realistic setting for the comparability of the measurements as opposed to young individuals. The time elapsed from surgery was six months to one year, there were no posterior capsule opacities, all subjects were implanted with the same PMMA lens, had best-corrected Snellen visual acuity 1.0, and the signal strength of the OCT images was also excellent. Thus, the effect of the posterior lens capsule opacification on the OCT scan, which consists primarily of a loss of signal and, consequently, of intraretinal detail, was not in place for any of the patients included in our study. Table 1 shows the

**Table 1** Inclusion and exclusion criteria for all participants and the clinical examinations performed.

| Inclusion criteria  |
|---|
| Best-corrected Snellen visual acuity of 20/20                                   |
| Preoperative spherical and cylindrical correction within $\pm 3.0$ diopters (D) |
| Exclusion criteria  |
| The presence of any retinal disease including glaucoma                          |
| The presence of systemic diseases except for controlled hypertension            |
| Clinical examinations   |
| Best corrected visual acuity (BCVA)   |
| Assessment of intraocular pressure (IOP)  |
| Slit lamp biomicroscopy   |
| Binocular ophthalmoscopy after pupil dilatation                                 |

inclusion and exclusion criteria for all participants along with the clinical examinations performed. All subjects were treated in accordance with the tenets of the Declaration of Helsinki. Informed consent was obtained from all participants in this study.

StratusOCT and RTVue examinations were performed on each eye by the same examiner and with intervals of  $\sim 10$  min. StratusOCT measurements were performed using the macular thickness map (MTM) protocol. This protocol consists of six radial scan lines centered on the fovea, each having a 6-mm transverse length. In order to obtain the best image quality, focusing and optimization settings were controlled and scans were accepted only if the signal strength (SS) was  $>6$  (preferably 9–10).<sup>11</sup> Scans with foveal decentration [i.e., with center-point thickness standard deviation (SD)  $> 10\%$ ] were repeated. The mean SD percentage of the center-point thickness was  $4.96 \pm 2.58\%$  for all scans that were accepted. StratusOCT raw data were exported and analyzed using OCTRIMA. Segmentation errors were manually corrected using the manual correction tool provided by OCTRIMA. MM5 and MM6 protocols were performed for RTVue measurements. MM5 protocol consists of a dense ( $5 \times 5$ )-mm grid of linear scans around the macula. MM6 protocol consists of 12 radial lines centered on the fovea with a 6-mm transverse length, similar to the Stratus MTM protocol. According to the Advanced Imaging for Glaucoma Study recommendations, RTVue scans with a signal strength index (SSI)  $\geq 45$  (range: 48.9–82.7) were considered.<sup>18</sup>

It is worth mentioning that the StratusOCT system images the outer retinal layers (RPE-photoreceptor complex) as two hyperreflective bands: (i) the photoreceptor IS and (ii) the RPE.<sup>19,20</sup> The segmentation software of the StratusOCT system uses the anterior border of the first or innermost hyperreflective band as the border of the outer retina for calculating total RT.<sup>21</sup> OCTRIMA calculates total RT as the distance between the vitreoretinal interface (ILM) and the anterior boundary of the second hyperreflective band corresponding to the OS/RPE junction. On the other hand, RT measurements of RTVue are taken between the ILM and the edge defined by the mean value of the maximum reflectance of the RPE in order to avoid detection errors at the RPE's outer border (personal information from the manufacturer, Optovue Inc., Fremont, California).

RT measured by StratusOCT, MM5 and MM6 protocols was compared for each of the nine early treatment diabetic retinopathy study (ETDRS) subfields with corresponding OCTRIMA results by analysis of variance (ANOVA) followed by Dunnett *post hoc* test with comparisons made to OCTRIMA results. The exact location of regions R1–9 is described in detail in Table 2.<sup>22</sup> Because the MM5 protocol uses a scan length of 5 mm, only the foveal and pericentral regional (R1–R5) data were used in the analyses. Paired t-test was performed to compare the thickness of the GCC measured by RTVue using the MM6 protocol and OCTRIMA with the exclusion of R1 because ganglion cells are not present in the area of the foveal pit. The correlations between the methods were calculated using Pearson correlation coefficients. Because the sampling is different at each ETDRS region, due to different radial spoke patterns used in the scanning protocols of Stratus and RTVue (MM6 protocol), a weighted mean thickness (WMT) was calculated instead of averaging RT results in the nine ETDRS regions.<sup>23</sup> The WMT represents an interpolated weighted average for all protocols. For each eye, WMT

**Table 2** Retinal thickness values in each ETDRS subfield by each software and the differences between the measurements. Data are presented as mean  $\pm$  SD (in micrometers). SD: standard deviation. WMT: weighted mean thickness.

|                     | Mean regional thickness |              |              |              | Mean difference of regional thickness |                         |                                      |                          |
|---------------------|-------------------------|--------------|--------------|--------------|---------------------------------------|-------------------------|--------------------------------------|--------------------------|
|                     | OCTRIMA                 | RTVue MM6    | RTVue MM5    | Stratus      | OCTRIMA minus Stratus                 | OCTRIMA minus RTVue MM6 | OCTRIMA minus RTVue MM5 <sup>a</sup> | RTVue MM6 minus Stratus  |
| R1 (fovea)          | 245 $\pm$ 19            | 257 $\pm$ 20 | 259 $\pm$ 19 | 206 $\pm$ 21 | 39 $\pm$ 4 <sup>b</sup>               | -12 $\pm$ 8             | -14 $\pm$ 7                          | 51 $\pm$ 9 <sup>b</sup>  |
| R2 (inner superior) | 314 $\pm$ 16            | 312 $\pm$ 18 | 318 $\pm$ 14 | 269 $\pm$ 17 | 45 $\pm$ 2 <sup>b</sup>               | 2 $\pm$ 10              | -4 $\pm$ 11                          | 44 $\pm$ 10 <sup>b</sup> |
| R3 (inner nasal)    | 316 $\pm$ 16            | 312 $\pm$ 17 | 321 $\pm$ 17 | 274 $\pm$ 17 | 42 $\pm$ 5 <sup>b</sup>               | 4 $\pm$ 6               | -5 $\pm$ 5                           | 38 $\pm$ 10 <sup>b</sup> |
| R4 (inner inferior) | 310 $\pm$ 20            | 314 $\pm$ 12 | 312 $\pm$ 20 | 269 $\pm$ 24 | 42 $\pm$ 5 <sup>b</sup>               | -4 $\pm$ 10             | -2 $\pm$ 4                           | 46 $\pm$ 14 <sup>b</sup> |
| R5 (inner temporal) | 302 $\pm$ 16            | 309 $\pm$ 15 | 304 $\pm$ 18 | 257 $\pm$ 17 | 45 $\pm$ 4 <sup>b</sup>               | -7 $\pm$ 7              | -2 $\pm$ 6                           | 52 $\pm$ 7 <sup>b</sup>  |
| R6 (outer superior) | 282 $\pm$ 18            | 257 $\pm$ 18 | —            | 228 $\pm$ 21 | 54 $\pm$ 8 <sup>b</sup>               | 25 $\pm$ 9 <sup>b</sup> | —                                    | 29 $\pm$ 11 <sup>b</sup> |
| R7 (outer nasal)    | 286 $\pm$ 14            | 268 $\pm$ 14 | —            | 243 $\pm$ 16 | 42 $\pm$ 6 <sup>b</sup>               | 18 $\pm$ 7 <sup>c</sup> | —                                    | 25 $\pm$ 11 <sup>b</sup> |
| R8 (outer inferior) | 260 $\pm$ 16            | 265 $\pm$ 11 | —            | 223 $\pm$ 16 | 36 $\pm$ 8 <sup>b</sup>               | -5 $\pm$ 8              | —                                    | 42 $\pm$ 12 <sup>b</sup> |
| R9 (outer temporal) | 258 $\pm$ 17            | 265 $\pm$ 14 | —            | 213 $\pm$ 17 | 45 $\pm$ 4 <sup>b</sup>               | -7 $\pm$ 6              | —                                    | 52 $\pm$ 6 <sup>b</sup>  |
| Mean thickness      | 286 $\pm$ 15            | 284 $\pm$ 13 | 303 $\pm$ 15 | 242 $\pm$ 15 | 43 $\pm$ 8 <sup>b</sup>               | 2 $\pm$ 13              | 48 $\pm$ 9                           | 42 $\pm$ 14 <sup>b</sup> |
| WMT                 | 279 $\pm$ 15            | 274 $\pm$ 13 | —            | 235 $\pm$ 16 | 44 $\pm$ 3 <sup>b</sup>               | 5 $\pm$ 4               | —                                    | 39 $\pm$ 6 <sup>b</sup>  |

<sup>a</sup>OCTRIMA and RTVue MM5 WMT results were not compared because of the different number of regions analyzed.

<sup>b</sup> $p < 0.01$  by Dunnett *post hoc* test.

<sup>c</sup> $p < 0.05$  by Dunnett *post hoc* test.

was generated using the following:

$$\text{WMT} = \frac{R1}{36} + \frac{R2 + R3 + R4 + R5}{18} + \frac{(R6 + R7 + R8 + R9) \times 3}{16}$$

Bland-Altman plots were constructed to assess agreement in WMT calculations. The systematic bias between RTVue and StratusOCT's WMT calculations was analyzed by fitting a linear regression for the difference of the two OCT techniques versus the average of the two WMT values. The corresponding 95% confidence interval (CI) of the mean difference and the slope of the Bland-Altman regression line were calculated in order to assess whether the differences between the two OCT techniques were statistically significant. Statistical analyses were performed using Statistica 8.0 Software (Statsoft Inc., Tulsa, Oklahoma). The level of significance was set at 5%.

### 3 Results

A high correlation was observed for regional RT when comparing OCTRIMA to RTVue MM5 and MM6 protocols (Pearson correlation coefficients range: 0.93–0.97 and 0.82–0.94, respectively, data not shown). Similarly, a high correlation was obtained for the regional GCC measurements when comparing OCTRIMA to RTVue MM6 protocol (Pearson correlation coefficients range: 0.73–0.88, data not shown).

ANOVA followed by Dunnett *post hoc* test showed no significant differences in regional thickness measurements by the MM6 protocol between OCTRIMA and RTVue except for

ETDRS regions R6 and R7. The mean difference in RT measurements between OCTRIMA, MM6 and MM5 protocols was  $< 7 \mu\text{m}$  in each ETDRS region except for R1, R6, and R7 (see Table 2). OCTRIMA produced significantly thicker

**Table 3** Mean GCC thickness values measured in each ETDRS subfield by OCTRIMA and RTVue MM6 protocol. For the description of R2-9 location, see Table 2. Data are presented as mean  $\pm$  SD (micrometers). SD: standard deviation. WMT: weighted mean thickness.

|     | OCTRIMA      | RTVue MM6    | OCTRIMA minus RTVue MM6  |
|-----|--------------|--------------|--------------------------|
| R2  | 114 $\pm$ 13 | 126 $\pm$ 12 | -12 $\pm$ 8 <sup>b</sup> |
| R3  | 114 $\pm$ 12 | 122 $\pm$ 12 | -8 $\pm$ 7 <sup>b</sup>  |
| R4  | 114 $\pm$ 16 | 125 $\pm$ 11 | -11 $\pm$ 9 <sup>b</sup> |
| R5  | 105 $\pm$ 13 | 119 $\pm$ 11 | -14 $\pm$ 9 <sup>b</sup> |
| R6  | 106 $\pm$ 14 | 93 $\pm$ 10  | 13 $\pm$ 8 <sup>b</sup>  |
| R7  | 112 $\pm$ 13 | 99 $\pm$ 8   | 13 $\pm$ 9 <sup>b</sup>  |
| R8  | 90 $\pm$ 12  | 96 $\pm$ 7   | -6 $\pm$ 8 <sup>a</sup>  |
| R9  | 87 $\pm$ 10  | 95 $\pm$ 7   | -8 $\pm$ 7 <sup>b</sup>  |
| WMT | 99 $\pm$ 13  | 99 $\pm$ 10  | 0 $\pm$ 5                |

<sup>a</sup> $p < 0.01$  by paired *t*-test compared to OCTRIMA measurements.

<sup>b</sup> $p < 0.05$  by paired *t*-test compared to OCTRIMA measurements.

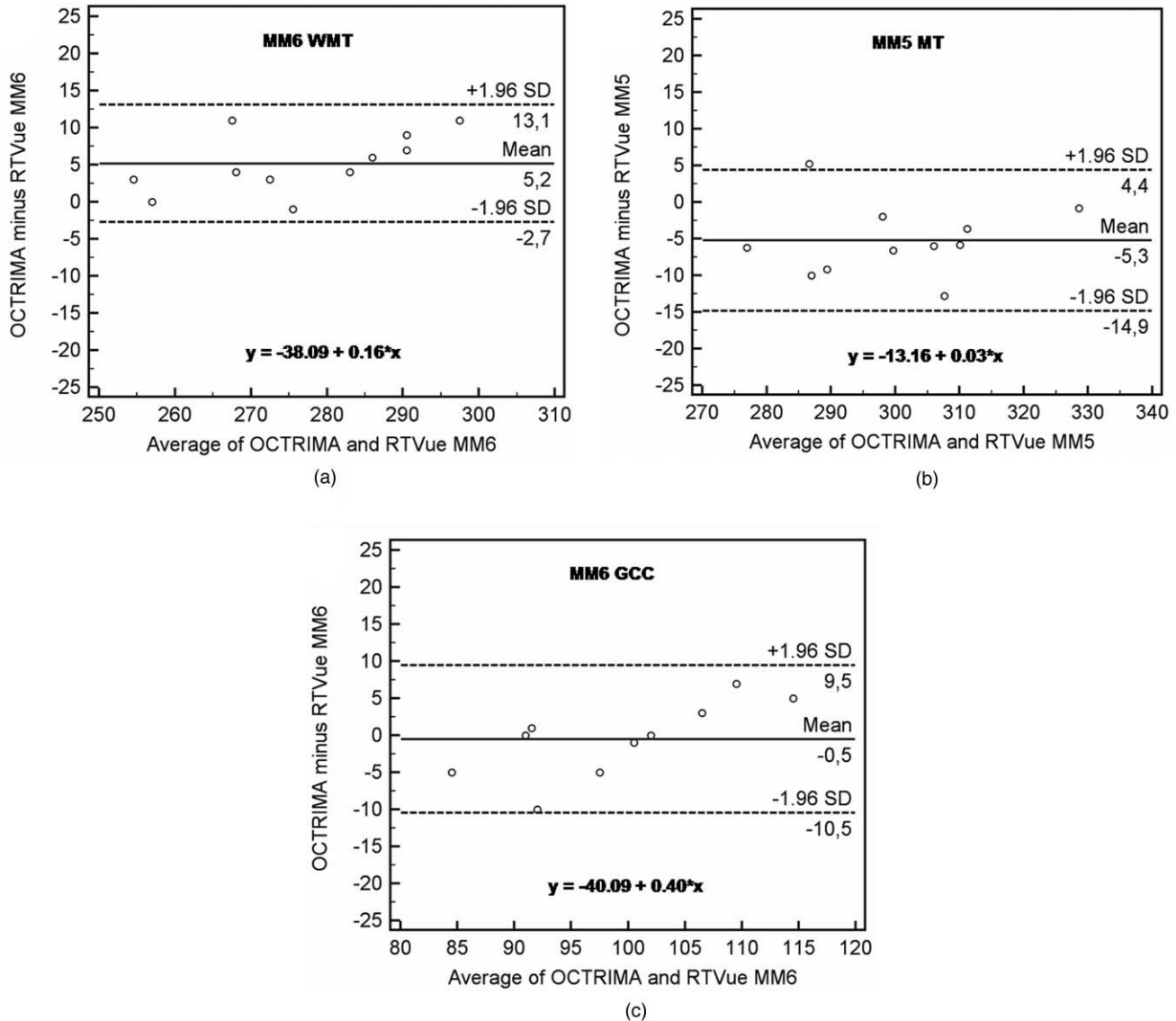


**Fig. 1** Bland-Altman plots comparison between OCTRIMA and RTVue. Values on the horizontal axis correspond to the mean of the two observed values by the two methods in micrometers. Values on the vertical axis correspond to the difference of the two observed values by the two methods in micrometers. The equation of the regression line is presented in each image. (a) Comparison of total RT measurements between OCTRIMA and RTVue using the MM6 protocol. Weighted mean total RT (WMT) was calculated for each patient for OCTRIMA and RTVue measurements. (b) Comparison of mean RT measurements (MT) between OCTRIMA and RTVue using the MM5 protocol. (c) Comparison of GCC measurements between OCTRIMA and RTVue using the MM6 protocol. Weighted mean GCC thickness was calculated for each patient for OCTRIMA and RTVue measurements. GCC thickness was calculated with the exclusion of the thickness values of R1 as ganglion cells are not present in the area of the foveal pit.

measurements for R6 and R7. In the case of the GCC thickness measurements, the mean difference range was from 6.3 to 12.4  $\mu\text{m}$  (see Table 3). GCC measurements were significantly thicker for the MM6 protocol, except for R6 and R7 where OCTRIMA produced thicker results.

Bland-Altman plots for the WMT difference between OCTRIMA and RTVue MM6 protocol and the average total RT between OCTRIMA and RTVue MM5 protocol are shown in Fig. 1. The difference in weighted mean GCC thickness between OCTRIMA and RTVue MM6 protocols are also shown in Fig. 1. The intercept of the Bland-Altman regression line corresponds to the mean difference between the two methods at zero thickness. This metric is not plausible; thus instead of intercepts,

Table 4 shows the statistically equivalent difference between the observed means. As Table 4 shows, the MM6 protocol gives a significantly smaller WMT than OCTRIMA, whereas MM5 gives significantly thicker results. The difference is at the level of the axial resolution of FD-OCT in both cases and corresponds to  $<2\%$  of mean RT, which is not clinically significant. There was no statistical difference for WMT results obtained for the GCC. However, it should be noted that the slope computation gave a significant result for the Bland-Altman plot of the GCC measurements. This particular result indicates that the RTVue algorithm overestimates low thickness values and underestimates high GCC thickness values compared to the OCTRIMA algorithm. The average GCC thickness difference between the

**Table 4** Comparative Bland-Altman analysis of OCTRIMA and RTVue measurements. The slope measure is the slope of the linear regression fitted to the Bland-Altman transformed data (see Fig. 1). Mean difference is calculated for OCTRIMA minus RTVue weighted mean thickness (WMT) results in the case of the MM6 protocol, while average RT was calculated in the case of the MM5 protocol as outer macular regions (R6–9) were not included in the comparison because of the different scan lengths.

|                                 | Mean difference<br>( $\mu\text{m}$ ) | Standard deviation<br>( $\mu\text{m}$ ) | 95% confidence<br>intervals ( $\mu\text{m}$ ) |       | Slope | 95% confidence<br>intervals |       |
|---------------------------------|--------------------------------------|---|---|-------|-------|-----------------------------|-------|
|                                 |                                      |   | Lower   | Upper |       | Lower                       | Upper |
| RT WMT (MM6 versus OCTRIMA)     | 5.18                                 | 3.88                                    | 2.58  | 7.79  | 0.16  | -0.01                       | 0.32  |
| Average RT (MM5 versus OCTRIMA) | -5.25                                | 4.96                                    | -8.54   | -1.96 | 0.03  | -0.22                       | 0.27  |
| GCC WMT (MM6 versus OCTRIMA)    | -0.42                                | 5.58                                    | -4.1  | 3.25  | 0.40  | 0.09                        | 0.71  |

two methods was  $3.74 \mu\text{m}$  (95% CI  $-1.98, +9.48$ ) when the thickness was  $<100$  micrometer and  $-2.66 \mu\text{m}$  (95% CI  $-6.47, +1.12$ ) when the thickness was  $>100$  micrometer.

#### 4 Discussion

Our results have shown good correlation between the total RT and GCC thickness measurement calculations of RTVue FD-OCT and OCTRIMA. On the other hand, both RTVue MM6 protocol and OCTRIMA measured significantly higher total RT values than StratusOCT. In our study, the RTVue's MM6 protocol was found to measure the retina  $42 \pm 14 \mu\text{m}$  thicker compared to StratusOCT algorithm's results. Furthermore, we found a  $43 \pm 8 \mu\text{m}$  mean difference between total RT values measured by OCTRIMA derived from StratusOCT images. These comparable results are due to similar boundary detections because the RT on RTVue images is calculated between the ILM and the edge defined by the mean value of the maximum reflectance of the RPE (see Fig. 2) and OCTRIMA measures total RT as the distance between the ILM and the inner border of the OS/RPE junction (defined as "true retinal thickness" by Hee<sup>24</sup>) (see Fig. 2). On the contrary, the algorithm of StratusOCT uses the anterior border of the innermost hyperreflective band as the border of the outer retina for calculating total RT.<sup>21,25</sup> Recent studies have shown that currently available FD-OCT devices are all giving significantly higher RT measurements than StratusOCT because of different assumptions considered for the detection of the outer retinal boundary, making the comparison of data obtained by different devices difficult (see Table 5). These differences also hinder the adequate evaluation of the performance of FD-OCT to detect the progression of disease.

The good correlation that was observed in our study emphasizes the capability of comparable retinal measurements by FD-OCT and StratusOCT-derived segmentation using the OCTRIMA software. As a potential weakness, our study did not include eyes with macular pathology (e.g., with macular edema or chorioretinal disorders), where the larger sampling density of FD-OCT could have played a better role in obtaining more precise measurements. However, we believe that our results can still be of value when assessing macular alterations with mild and roughly generalized macular changes, like those observed in glaucoma, neurodegenerative diseases, or inherited macular disorders, where in early phases macular structure may

seemingly be unaffected.<sup>26–29</sup> Nonetheless, future studies will explore the capability of OCTRIMA for OCT images showing macular alterations.

Bland-Altman plots showed that the weighted mean total RT measured by OCTRIMA is, on average,  $5 \mu\text{m}$  higher than that measured by RTVue using the MM6 protocol and is, on average,  $5 \mu\text{m}$  lower than that measured by RTVue using the MM5 protocol, which both are below the axial resolution of the devices (see Fig. 1). The explanation for the comparable differences might be that the location of the mean value of

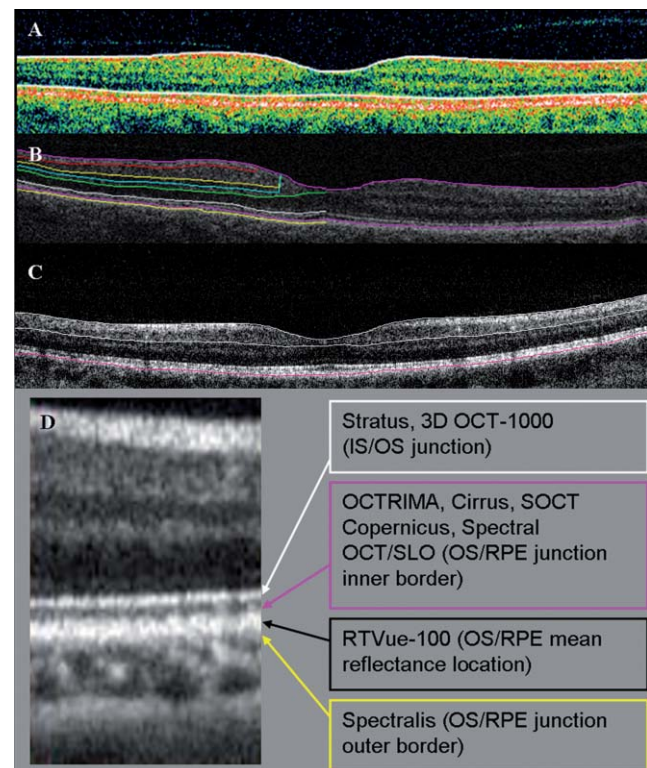


**Fig. 2** The outer retinal boundary detection of (a) Stratus, (b) OCTRIMA, and (c) RTVue OCT. For better visualization, the outer retinal boundary of RTVue is highlighted manually in magenta color, similarly to that seen with OCTRIMA. (d) An enlarged part of a FD-OCT image demonstrating the outer retinal border delineation of various OCT devices and OCTRIMA. (Color online only.)

**Table 5** Fourier-domain OCT reports on the difference measured compared to StratusOCT in healthy eyes. SD values are presented only where the original paper contained the relevant data.

| FD-OCT device    | Difference measured from StratusOCT <sup>a</sup> | No. of Eyes | Author  |
|------------------|--|-------------|---|
| Spectralis       | 77 $\mu\text{m}^{\text{b}}$                      | 20          | Wolf-Schnurrbusch <i>et al.</i> <sup>34</sup> |
| Spectralis       | 69.3 $\pm$ 15.3 $\mu\text{m}^{\text{c}}$         | 10          | Han and Jaffe <sup>35</sup>                   |
| Cirrus           | 65 $\mu\text{m}^{\text{b}}$                      | 20          | Wolf-Schnurrbusch <i>et al.</i> <sup>34</sup> |
| Cirrus           | 62.3 $\pm$ 7.3 $\mu\text{m}^{\text{c}}$          | 13          | Legarreta <i>et al.</i> <sup>36</sup>         |
| Cirrus           | 60.4 $\mu\text{m}^{\text{d}}$                    | 50          | Kakinoki <i>et al.</i> <sup>37</sup>          |
| Cirrus           | 60.0 $\pm$ 9.0 $\mu\text{m}^{\text{c}}$          | 11          | Durbin <i>et al.</i> <sup>38</sup>            |
| Cirrus           | 53.8 $\pm$ 16.9 $\mu\text{m}^{\text{c}}$         | 12          | Han and Jaffe <sup>35</sup>                   |
| Cirrus           | 43 $\mu\text{m}^{\text{d}}$                      | 28          | Menke <i>et al.</i> <sup>2</sup>              |
| Cirrus           | 41.9 $\mu\text{m}^{\text{c}}$                    | 55          | Kiernan <i>et al.</i> <sup>39</sup>           |
| OCTRIMA          | 43 $\pm$ 8 $\mu\text{m}^{\text{d}}$              | 11          | Tatrai <i>et al.</i> (present study)          |
| RTVue-100        | 42 $\pm$ 14 $\mu\text{m}^{\text{d}}$             | 11          | Tatrai <i>et al.</i> (present study)          |
| RTVue-100        | 35 $\mu\text{m}^{\text{b}}$                      | 20          | Wolf-Schnurrbusch <i>et al.</i> <sup>34</sup> |
| RTVue-100        | 14.89 $\pm$ 13.2 $\mu\text{m}^{\text{c}}$        | 32          | Huang <i>et al.</i> <sup>31</sup>             |
| RTVue-100        | 8 $\mu\text{m}^{\text{d}}$                       | 28          | Menke <i>et al.</i> <sup>2</sup>              |
| SOCT Copernicus  | 37 $\mu\text{m}^{\text{b}}$                      | 20          | Wolf-Schnurrbusch <i>et al.</i> <sup>34</sup> |
| Spectral OCT/SLO | 32 $\mu\text{m}^{\text{b}}$                      | 20          | Wolf-Schnurrbusch <i>et al.</i> <sup>34</sup> |
| Spectral OCT/SLO | 30.9 $\mu\text{m}^{\text{d}}$                    | 52          | Forte <i>et al.</i> <sup>40</sup>             |
| 3D OCT-1000      | 3.2 $\mu\text{m}^{\text{d}}$                     | 35          | Leung <i>et al.</i> <sup>41</sup>             |

<sup>a</sup>Data are presented as mean  $\pm$  SD.

<sup>b</sup>Central macular thickness.

<sup>c</sup>Mean foveal thickness.

<sup>d</sup>Mean retinal thickness (calculated by averaging the differences in the 9 ETDRS regions).

the maximum reflectance of the RPE calculated by RTVue and used to define the outer border of the retina is closely located to the inner border of the OS/RPE junction. Therefore, since slope computations for the plots gave no significant alteration from zero, the small differences between the two methods used to calculate total RT measurements in RTVue and OCTRIMA are hardly distinguishable and not biased by the methodology used in the analysis. Correspondingly, high correlations for the regional RT measurements were obtained when these measurements were compared between OCTRIMA and RTVue using MM5 and MM6 protocols.

It should be noted that RT measurements obtained in R1 by the MM5 and MM6 protocols of RTVue were approximately 12–14  $\mu\text{m}$  higher than measurements obtained with OCTRIMA, however not reaching a statistical difference. The reason for this difference is not clear because both StratusOCT and RTVue scans were carefully centered; therefore, the difference is unlikely to have been caused by decentration artifacts. However, differences in axial resolution and calibration techniques might

contribute to thickness measurement differences. Besides, mean RT values were generated with different scan protocols with the sampling density being higher by the RTVue MM6 protocol (12 radial scans) compared to StratusOCT (six radial scans), which might also contribute to the difference between the thickness measurements in R1.

Despite the high correlation of RT measurements, the RTVue results obtained with the MM6 protocol in regions R6 and R7 produced significantly thinner results than OCTRIMA, by approximately 18–25  $\mu\text{m}$ . A possible error source could have been the incorrect scanning distance and the resultant changes of the incident scanning beams when using the RTVue OCT device. Therefore, a study was performed by our group to assess the effect of wrong distance scanning on boundary detection errors on the periphery of the RTVue scans and the resultant errors on the thickness measurements.<sup>30</sup> Briefly, 10 eyes of 10 healthy subjects were examined with the same RTVue OCT device using the MM5 protocol in two sessions to scan the macula. First, the device was set at 3.5 cm from the eye in order to obtain

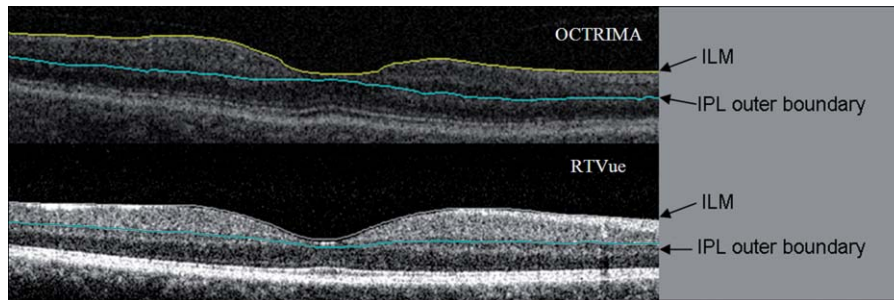


**Fig. 3** (a) OCTRIMA and (b) RTVue segmentation results obtained for the total retinal thickness and the GCC in a healthy patient. The outer border of the GCC is highlighted manually with blue color, similarly to that seen with OCTRIMA. Note that OCTRIMA segmentation results are overlaid on the StratusOCT raw image [see (a)]. (Color online only.)

detectable signal with low fundus image quality (“bad” scan distance setting), whereas in the second session a distance of  $\sim 2.5$  cm was set with a good quality fundus image (“good” scan distance setting). The score for inner and outer retinal boundary detection errors was calculated for five vertical and five horizontal selected scans of the MM5 grid protocol from each eye for both settings. The SSI was found to be significantly higher with “good” scan distance settings compared to “bad” scan distance settings. However, the number of retinal boundary detection errors in the central and peripheral regions and also the regional thickness measurements did not differ significantly between the two settings. Thus, we do not think that the differences in R6 and R7 were due to low SS in the peripheral regions or incorrect boundary detection. Accordingly, a possible explanation for the thickness differences could be related to a combination of different data sampling, instrumentation and light beam directionality (i.e., different incidence angle of the scanning beam in the upper and nasal region when scanning same eyes with different devices).

Interestingly, similar results were found by Huang *et al.* when comparing regional thickness measurements between StratusOCT and RTVue OCT.<sup>31</sup> They found that RTVue produced significantly higher RT measurements in each ETDRS region except for R8, where the difference was not significant, and R7 where StratusOCT produced thicker measurements than RTVue (as in our study). However, no explanation was provided for these differences. Particularly, R7 in the report by Huang *et al.*<sup>31</sup> should be thinner when measured with Stratus OCT because the outer retinal border in Stratus is assumed to be anteriorly located compared to the assumption in RTVue (which is at the level of the OS/RPE junction). Therefore, contradictory results are in place for these particular regions when using the RTVue as reported by Huang *et al.*<sup>31</sup> and our group. Taking into consideration that the anatomical properties of the macular regions in the periphery have been previously described as being thicker in the nasal than in the temporal macular area,<sup>22</sup> we suppose that thickness values measured by the RTVue device should have been higher in R6 and R7.

It is also of great interest that the software of the RTVue device enables the segmentation of the GCC in the macula, which might facilitate a more rigorous glaucoma analysis.<sup>32</sup> Certainly, OCTRIMA is also able to extract the GCC; therefore, we also compared the potentialities of the two algorithms (Fig. 3). A good correspondence between OCTRIMA and RTVue MM6 protocol was found; however, thickness values measured by the

RTVue device were 6–10  $\mu\text{m}$  higher in all but regions R6 and R7. Interestingly, GCC in subfields R6 and R7 was  $\sim 12$ - $\mu\text{m}$  thinner by the RTVue using the MM6 protocol, similarly to total RT values. This difference was less than that observed for the total RT; therefore, we assume it is not an isolated GCC or outer retinal boundary detection error. The above differences in GCC measurements should be carefully considered in clinical settings exploring eye diseases affecting the ganglion cells, such as glaucoma and neurodegenerative diseases. The small mean difference of 1  $\mu\text{m}$  shown by the Bland-Altman plot of WMT results might be misleading because it could be due to the results in R6 and R7 influencing the calculation of the mean as the differences of the regions may outweigh each other. Also, the slope computation of the plot’s linear regression showed a significant difference, which implies a thickness-dependent bias of the measurements; however, this bias is relatively small. Therefore, care must be taken when comparing GCC results from different OCT devices and further investigations are needed to better understand the background of these differences.

In summary, we found that measurements with the StratusOCT showed the lowest RT values, whereas measurements with the RTVue OCT and StratusOCT-derived images assessed by OCTRIMA yielded the highest ones. These discrepancies were based on differences in retinal segmentation algorithms, sampling data, and instrumentation. In addition, a high correspondence of RT measurements between FD-OCT and StratusOCT-derived images assessed by OCTRIMA was demonstrated. Despite the worse resolution of TD-OCT, we could achieve a high correspondence of retinal layer segmentation with FD-OCT in elderly subjects who are supposed to have bad fixation cooperation. Weighted mean total RT data were shown to have a high correlation, while regional differences might still exist. The measurements of the GCC should also be compared to care because there is a marked regional difference between OCTRIMA and RTVue using the MM6 protocol, which might be slightly biased by the thickness of the GCC layer. These differences were most probably based on differences in retinal segmentation algorithms, sampling, calibration, and axial resolution.

An agreement between ophthalmologists and developers is needed in order to standardize OCT RT measurements. However, the use of custom-built segmentation algorithms along with open-source image applications could also facilitate the transformation of data obtained by different devices.<sup>33</sup> In view of the higher price of FD-OCT systems and the use of TD-OCT



worldwide, we believe our OCTRIMA software can be of substantial value in future studies of macular pathophysiology and might also perform well for FD-OCT images in the future.

### Acknowledgments

The authors thank Dr. László Tóthfalusi for his valuable help with the statistical analyses presented in the manuscript. This study was supported in part by a Juvenile Diabetes Research Foundation Grant, a NIH Center Grant No. P30-EY014801, by an unrestricted grant to the University of Miami from Research to Prevent Blindness, Inc., and by the Zsigmond Diabetes Fund of the Hungarian Academy of Sciences. The University of Miami and Dr. Cabrera DeBuc hold a pending patent used in the study and have the potential for financial benefit from its future commercialization. All other authors of the paper report no disclosures.

### References

1. D. Huang, E. A. Swanson, C. P. Lin, J. S. Schuman, W. G. Stinson, W. Chang, M. R. Hee, T. Flotte, K. Gregory, C. A. Puliafito, and J. G. Fujimoto, "Optical coherence tomography," *Science* **254**(5035), 1178–1181 (1991).
2. M. N. Menke, S. Dabov, and V. Sturm, "Comparison of three different optical coherence tomography models for total macular thickness measurements in healthy controls," *Ophthalmologica* **223**(6), 352–356 (2009).
3. R. A. Costa, M. Skaf, L. A. Melo, Jr., D. Calucci, J. A. Cardillo, J. C. Castro, D. Huang, and M. Wojtkowski, "Retinal assessment using optical coherence tomography," *Prog Retin. Eye Res.* **25**(3), 325–353 (2006).
4. J. F. de Boer, B. Cense, B. H. Park, M. C. Pierce, G. J. Tearney, and B. E. Bouma, "Improved signal-to-noise ratio in spectral-domain compared with time-domain optical coherence tomography," *Opt. Lett.* **28**(21), 2067–2069 (2003).
5. W. Drexler and J. G. Fujimoto, "State-of-the-art retinal optical coherence tomography," *Prog. Retin. Eye Res.* **27**(1), 45–88 (2008).
6. M. E. van Velthoven, D. J. Faber, F. D. Verbraak, T. G. van Leeuwen, and M. D. de Smet, "Recent developments in optical coherence tomography for imaging the retina," *Prog. Retin. Eye Res.* **26**(1), 57–77 (2007).
7. D. U. Bartsch, X. Gong, C. Ly, and W. R. Freeman, "Optical coherence tomography: interpretation artifacts and new algorithm," *Proc. SPIE* **5370**, 2140–2151 (2004).
8. R. Ray, S. S. Stinnett, and G. J. Jaffe, "Evaluation of image artifact produced by optical coherence tomography of retinal pathology," *Am. J. Ophthalmol.* **139**(1), 18–29 (2005).
9. S. R. Sadda, S. Joeres, Z. Wu, P. Updike, P. Romano, A. T. Collins, and A. C. Walsh, "Error correction and quantitative subanalysis of optical coherence tomography data using computer-assisted grading," *Invest. Ophthalmol. Vis. Sci.* **48**(2), 839–848 (2007).
10. S. R. Sadda, Z. Wu, A. C. Walsh, L. Richine, J. Dougall, R. Cortez, and L. D. LaBree, "Errors in retinal thickness measurements obtained by optical coherence tomography," *Ophthalmology* **113**(2), 285–293 (2006).
11. G. M. Somfai, H. M. Salinas, C. A. Puliafito, and D. C. Fernandez, "Evaluation of potential image acquisition pitfalls during optical coherence tomography and their influence on retinal image segmentation," *J. Biomed. Opt.* **12**(4), 041209 (2007).
12. D. Cabrera Fernández, H. M. Salinas, and C. A. Puliafito, "Automated detection of retinal layer structures on optical coherence tomography images," *Opt. Express* **13**(25), 10200–10216 (2005).
13. W. Gao, S. Ranganathan, E. Tátrai, G. M. Somfai, and D. C. Fernandez, "Development of a graphic user interface as an additional tool of diagnostic differentiation of retinal tissue using optical coherence tomography," *Invest. Ophthalmol. Vis. Sci.* **49**(5), 1891 (2008).
14. D. C. Debuc, H. M. Salinas, S. Ranganathan, E. Tátrai, W. Gao, M. Shen, J. Wang, G. M. Somfai, and C. A. Puliafito, "Improving image segmentation performance and quantitative analysis via a computer-aided grading methodology for optical coherence tomography retinal image analysis," *J. Biomed. Opt.* **15**(4), 046015 (2010).
15. D. C. DeBuc, G. M. Somfai, S. Ranganathan, E. Tátrai, M. Ferencz, and C. A. Puliafito, "Reliability and reproducibility of macular segmentation using a custom-built coherence tomography retinal image analysis software," *J. Biomed. Opt.* **14**(6), 064023 (2009).
16. C. Tappeiner, D. Barthelmes, M. H. Abegg, S. Wolf, and J. C. Fleischhauer, "Impact of optic media opacities and image compression on quantitative analysis of optical coherence tomography," *Invest. Ophthalmol. Vis. Sci.* **49**(4), 1609–1614 (2008).
17. M. E. J. van Velthoven, M. H. Van Der Linden, M. D. de Smet, D. J. Faber, and F. D. Verbraak, "Influence of cataract on optical coherence tomography image quality and retinal thickness," *Br. J. Ophthalmol.* **90**(10), 1259–1262 (2006).
18. *AIGS manual of Procedures*, [http://www.aigstudy.net/fileadmin/aigs\\_upload/docs/ManualOfProcedures5.pdf](http://www.aigstudy.net/fileadmin/aigs_upload/docs/ManualOfProcedures5.pdf), last accessed 31 March 2011.
19. G. S. Hageman, M. F. Marmor, X. Y. Yao, and L. V. Johnson, "The interphotoreceptor matrix mediates primate retinal adhesion," *Arch. Ophthalmol.* **113**(5), 655–660 (1995).
20. B. Sander, M. Larsen, L. Thrane, J. L. Hougaard, and T. M. Jorgensen, "Enhanced optical coherence tomography imaging by multiple scan averaging," *Br. J. Ophthalmol.* **89**(2), 207–212 (2005).
21. R. A. Costa, D. Calucci, M. Skaf, J. A. Cardillo, J. C. Castro, L. A. Melo, Jr., M. C. Martins, and P. K. Kaiser, "Optical coherence tomography 3: automatic delineation of the outer neural retinal boundary and its influence on retinal thickness measurements," *Invest. Ophthalmol. Vis. Sci.* **45**(7), 2399–2406 (2004).
22. P. Massin, A. Erginay, B. Haouchine, A. B. Mehid, M. Paques, and A. Gaudric, "Retinal thickness in healthy and diabetic subjects measured using optical coherence tomography mapping software," *Eur. J. Ophthalmol.* **12**(2), 102–108 (2002).
23. P. Massin, E. Vicaut, B. Haouchine, A. Erginay, M. Paques, and A. Gaudric, "Reproducibility of retinal mapping using optical coherence tomography," *Arch. Ophthalmol.* **119**(8), 1135–1142 (2001).
24. M. R. Hee, "Automated measurements of retinal thickness with optical coherence tomography," *Am. J. Ophthalmol.* **140**(2), 350–351; author reply 351 (2005).
25. M. E. Pons and E. Garcia-Valenzuela, "Redefining the limit of the outer retina in optical coherence tomography scans," *Ophthalmology* **112**(6), 1079–1085 (2005).
26. A. Giovannini, G. Amato, and C. Mariotti, "The macular thickness and volume in glaucoma: an analysis in normal and glaucomatous eyes using OCT," *Acta Ophthalmol. Scand Suppl.* **236**, 34–36 (2002).
27. D. S. Greenfield, H. Bagga, and R. W. Knighton, "Macular thickness changes in glaucomatous optic neuropathy detected using optical coherence tomography," *Arch. Ophthalmol.* **121**(1), 41–46 (2003).
28. J. Hargitai, J. Zernant, G. M. Somfai, R. Vamos, A. Farkas, G. Salacz, and R. Allikmets, "Correlation of clinical and genetic findings in Hungarian patients with Stargardt disease," *Invest. Ophthalmol. Vis. Sci.* **46**(12), 4402–4408 (2005).
29. D. B. Hess, S. G. Asrani, M. G. Bhide, L. B. Enyedi, S. S. Stinnett, and S. F. Freedman, "Macular and retinal nerve fiber layer analysis of normal and glaucomatous eyes in children using optical coherence tomography," *Am. J. Ophthalmol.* **139**(3), 509–517 (2005).
30. G. M. Somfai, E. Tátrai, B. Varga, and D. Cabrera DeBuc, "The effect of scanning pitfalls on boundary detection errors and macular thickness measurements of the RTVue MM5 Protocol," *ARVO Meeting Abstracts* **51**(5), 4399 (2010).
31. J. Huang, X. Liu, Z. Wu, H. Xiao, L. Dustin, and S. Sadda, "Macular thickness measurements in normal eyes with time-domain and Fourier-domain optical coherence tomography," *Retina* **29**(7), 980–987 (2009).
32. O. Tan, V. Chopra, A. T. Lu, R. Varma, and D. Huang, "Glaucoma diagnosis by mapping the macula with Fourier domain optical coherence tomography," *Invest. Ophthalmol. Vis. Sci.* **48**(5), 512 (2007).
33. G. Mylonas, C. Ahlers, P. Malamos, I. Golbaz, G. Deak, C. Schutze, S. Sacu, and U. Schmidt-Erfurth, "Comparison of retinal thickness measurements and segmentation performance of four different spectral and time domain OCT devices in neovascular age-related macular degeneration," *Br. J. Ophthalmol.* **93**(11), 1453–1460 (2009).

34. U. E. Wolf-Schnurrbusch, L. Ceklic, C. K. Brinkmann, M. Iliev, M. Frey, S. P. Rothenbuehler, V. Enzmann, and S. Wolf, "Macular thickness measurements in healthy eyes using six different optical coherence tomography instruments," *Invest. Ophthalmol. Vis. Sci.* **50**(7), 3432–3437 (2009).
35. I. C. Han and G. J. Jaffe, "Comparison of spectral- and time-domain optical coherence tomography for retinal thickness measurements in healthy and diseased eyes," *Am. J. Ophthalmol.* **147**(5), 847–858 (2009).
36. J. E. Legarreta, G. Gregori, O. S. Punjabi, R. W. Knighton, G. A. Lalwani, and C. A. Puliafito, "Macular thickness measurements in normal eyes using spectral domain optical coherence tomography," *Ophthalm. Surg. Lasers Imaging* **39**(4 Suppl), S43–49 (2008).
37. M. Kakinoki, O. Sawada, T. Sawada, H. Kawamura and M. Ohji, "Comparison of macular thickness between Cirrus HD-OCT and Stratus OCT," *Ophthalm. Surg. Lasers Imaging* **40**(2), 135–140 (2009).
38. M. Durbin, T. Abunto, M. Chang, and B. Lujan, Retinal measurements: Comparison between Cirrus HD-OCT and Stratus OCT. Information Brochure, available at <http://www.zeiss.de/C1256C4F002FF302/EmbedTitelIntern/Cirrus-vs-Stratus-retinal-measurements-whitepaper/File/Cirrus-vs-Stratus-retinal-measurements-whitepaper.pdf> (2007).
39. D. F. Kiernan, S. M. Hariprasad, E. K. Chin, C. L. Kiernan, J. Rago, and W. F. Mieler, "Prospective comparison of cirrus and stratus optical coherence tomography for quantifying retinal thickness," *Am. J. Ophthalmol.* **147**(2), 267–275 e262 (2009).
40. R. Forte, G. L. Cennamo, M. L. Finelli, and G. de Crecchio, "Comparison of time domain Stratus OCT and spectral domain SLO/OCT for assessment of macular thickness and volume," *Eye* **23**(11), 2071–2078 (2008).
41. C. K. Leung, C. Y. Cheung, R. N. Weinreb, G. Lee, D. Lin, C. P. Pang, and D. S. Lam, "Comparison of macular thickness measurements between time domain and spectral domain optical coherence tomography," *Invest. Ophthalmol. Vis. Sci.* **49**(11), 4893–4897 (2008).